



# VentQsys: Low-cost open IoT system for CO<sub>2</sub> monitoring in classrooms

Rafael Fayos-Jordan<sup>1</sup> · Jaime Segura-Garcia<sup>1</sup> · Antonio Soriano-Asensi<sup>1</sup> · Santiago Felici-Castell<sup>1</sup> · Jose M. Felisi<sup>2</sup> · Jose M. Alcaraz-Calero<sup>3</sup>

Accepted: 6 September 2021  
© The Author(s) 2021

## Abstract

In educational context, a source of nuisance for students is carbon dioxide (CO<sub>2</sub>) concentration due to closed rooms and lack of ventilation or circulatory air. Also, in the pandemic context, ventilation in indoor environments has been proven as a good tool to control the COVID-19 infections. In this work, it is presented a low cost IoT-based open-hardware and open-software monitoring system to control ventilation, by measuring carbon dioxide (CO<sub>2</sub>), temperature and relative humidity. This system provides also support for automatic updating, auto-self calibration and adds some Cloud and Edge offloading of computational features for mapping functionalities. From the tests carried out, it is observed a good performance in terms of functionality, battery durability, compared to other measuring devices, more expensive than our proposal.

**Keywords** IoT · WSN · Spatial statistics · CO<sub>2</sub> · Open-source · Sustainability

## Abbreviations

TVOC	Total Volatile Organic Compounds	SARS-COV-2	Severe Acute Respiratory Syndrome
RH	Relative humidity	COVID-19	COronaVirus 2
NDIR	Non-Dispersive InfraRed	MCU	Micro-controller unit
UART	Universal asynchronous receiver-transmitter	EPROM	Erasable Programmable Read-Only Memory
ETSE	Escola Tècnica Superior d'Enginyeria (Engineering Technical School)	IoT	Internet of Things
		RPi	Raspberry Pi
		Wi-Fi	Wireless Fidelity (IEEE 802.11)
		OTA	Over the air
		OLED	Organic light-emitting diode
		RGB	Red-Green-Blue
		COPD	Chronic Obstructive Pulmonary Disease
		WSN	Wireless sensor network
		LTE	Long term evolution
		BLE	Bluetooth low energy

---

✉ Jaime Segura-Garcia  
jsegura@uv.es

Rafael Fayos-Jordan  
rafajor@uv.es

Antonio Soriano-Asensi  
ansoras@uv.es

Santiago Felici-Castell  
felici@uv.es

Jose M. Felisi  
josemanuel@g-agua.com

Jose M. Alcaraz-Calero  
jose.alcaraz-calero@uws.ac.uk

<sup>1</sup> Computer Science Department, Escola Tècnica Superior d'Enginyeria, Universitat de València, Burjassot 46100, Spain

<sup>2</sup> G-Agua (Tecnologia de la Gestió del Agua), SNLE, Riba-roja de Túria 46190, Spain

<sup>3</sup> School of Computing, Engineering and Physical Sciences, University of the West of Scotland, PA1 1LU Paisley, United Kingdom

## 1 Introduction

Carbon dioxide (CO<sub>2</sub>) is a colorless and odorless gas. It is naturally found in ambient air in concentrations ranging from 300 ppm to 550 ppm, depending on whether we measure in rural or urban environments. It is produced by (human and animal) breathing and burning fossil fuels. In the atmosphere, this gas produces the displacement of oxygen and in high concentrations (over 30,000 ppm), it can produce rapid breathing, confusion and asphyxiation, by reducing the oxygen concentration below 20% [7].

Actually  $CO_2$  is a great indicator of air quality, since it acts as a whistle blower for air renewal. It is known that from concentrations of more than 800 ppm in working environments, complaints due to odors begin to occur. However, the usual levels that we can find in an indoor environment will be related to different variables that affect this factor, such as outdoor air levels, indoor sources, occupancy levels and ventilation rates.

In addition, in the educational sector, high  $CO_2$  concentrations are a source of nuisance for students, due to closed rooms, lack of ventilation or circulatory air in classrooms [24] and they can affect the performance of the students. The educational authorities show some concerns, because with this situation not only the performance is compromised but also their health. Several studies have shown some relationship between the environmental pollution levels, in particular those related to  $CO_2$ , and some breathing diseases: hypercapnia, Chronic Obstructive Pulmonary Disease (COPD), etc. [7, 11].

Although there are some sensors able to monitor  $CO_2$  in indoor environments, their prices range from 100 to 300, and their networking abilities are limited to collect data (they only allow download data in csv or pdf format in the measurement device). In this work, our goal is to develop a configurable low-cost open-hardware and open-software IoT system (with nodes costing less than 70) to measure  $CO_2$  concentration by using a Non-Dispersive Infrared Absorption Spectroscopy (NDIR) sensor, measuring  $T$  and  $RH$  as well. Also, we aim to improve the performance of the system by adding different functionalities for upgrading [20], auto-self networked calibration, as well as include some computational offloading capabilities to Edge and Cloud for advance mapping functions.

This paper is structured as follows. First this introductory section has introduced the problem, explaining the context, the goal and after a section with some related works. Then, the materials and methods section explains the design and implementation of the node, as well the architecture of the IoT system to interconnect these nodes with external tools for control and management. The following section explains the measurement sessions done in different environments and the energy consumption performance evaluation done with the sensing node, discussing also these results. Finally, the conclusions section explains the lessons learnt and summarizes the innovations introduced.

## 2 Related work

In [28], authors measure  $CO_2$  concentration in different schools in Serbia. Their measurements exceed recommended concentrations, as over 800 ppm can generate sick building syndrome [27]. This syndrome is described

associated to different symptoms as: headache; eye, nose, or throat irritation; dry cough; dry or itchy skin; dizziness and nausea; difficulty in concentrating; fatigue; and sensitivity to odors.

In [16], authors found a correlation between the SARS virus spread and the sick building syndrome. Also in the SARS-COV-2 pandemic context, an increasing concern is raising about the virus spread, related to the fact that the probability of infection increases in indoor environments. This probability is proportional to the  $CO_2$  concentration [3, 15] and it is inversely related to the amount of ventilation. As ventilation is the air renovation, i.e. the exchange of potentially contaminated indoor air with outdoor air (theoretically free of virus), it allows the elimination of particles in suspension, which potentially can contain virus, and on its possible pathways [4]. This concern has evolved into recommendations, given by some Governments and research institutions [13, 18], for ventilation in school classrooms and indoor public places in order to reduce the probability of COVID-19 infections. This assertion is supported by [30], where the author concludes that indoor air quality control strategies can be integrated to reduce the risk of SARS-COV-2 infection.

The state of the art in environmental pollution issues is wide and many applications related to Wireless Sensor Networks (WSN) have been deployed. In [19], a survey on different applications of these networks is shown for real-time ambient air pollution monitoring and air quality in metropolitan areas. It must be noticed that these WSNs have been applied in different scenarios during the last two decades for different issues, such as lightning strike detection [17], or soundscape monitoring [21], etc.

It is worth mentioning that among the different aspects involved in this kind of systems for air quality monitoring, both the sensing part and the networking part are the predominant ones. On one hand, focusing on the sensing part, in [9], the authors carry out a performance evaluation of a number of low-cost consumer grade monitors and single-parameter sensors in detecting five indoor environmental parameters: particulate matter (PM or particle pollution),  $CO_2$ , Total Volatile Organic Compounds (TVOC), dry-bulb air ( $T$ ) and Relative Humidity ( $RH$ ). Their study shows that technological advancements have raised an opportunity for more effective indoor air quality control and management, suggesting that most of the tested monitors have the potential to be used to secure adequate indoor environments by triggering the right chain of actions. On the other hand, focusing on the networking part for environmental monitoring, in [5] are shown optimal WSN deployment models for air pollution monitoring. In [22], the authors describe a system for air quality monitoring in different cities. In this case, the authors, use ThingSpeak to collect data in the Cloud, using different communication

technologies in the WSN (i.e. Zigbee, Wifi, LTE and BLE). Also in [14], the authors develop a client-server system with LTE communication and with a set of sensors for measuring PM2.5 and PM10 (PM2007), VOCs, CO, CO<sub>2</sub>, temperature/humidity.

In [23], the authors develop a system for air quality monitoring and temperature (*T*) in classrooms, based on Z-Wave technology sending information to a central gateway. They study the well-being of pupils as it depends on indoor environmental quality and thermal comfort. Finally, in [2], the authors focus on Cloud computing and artificial intelligence developments in order to assist in the air monitoring process. In Table 1, we have summarized some qualitative features comparing our solution with other solutions from the state-of-the-art.

### 3 Materials and methods

In this section, the materials and methods used in the development of this IoT system are explained, as well as the architecture used.

#### 3.1 Node development

In the development of the sensing nodes, NodeMCU, a ESP8266-based platform, is used [20]. The NodeMCU is in charge of sampling and reading the CO<sub>2</sub> sensor outputs via UART communications with the selected CO<sub>2</sub> sensor, and of sending such values using WiFi-based communications. Two possible NodeMCUs models are supported in our prototype: Amica (with ESP-12E and chipset CP2102)[12] and Lolin (with ESP-12F and chipset CH340). The node is completed with a RGB led with common cathode to show directly the different levels in the next scale: low or green for values up to 800ppm, medium or blue for values between 800 and 1500ppm, and finally high or red for values greater than 1500ppm. Besides an OLED (organic

light-emitting diode) screen shows the values of the different parameters.

Our proposal is oriented to measure CO<sub>2</sub>, *T* and *RH*. We have used the so-called NDIR sensor, which is the most popular tool for CO<sub>2</sub> monitoring, that does not require analytical grade concentration readings. A NDIR sensor is a simple spectroscopic sensor based on an infrared source (lamp) with a sample chamber (or light tube), a light filter and an infrared detector, providing high accuracy. For this reason, our selection has been made separately with a MH-Z19 [31] (or optionally, MG811 which is based on solid electrolyte cell principle) and a DHT22 [1] (with an accuracy of 0.5°C for *T*, ranging from -40°C to 80°C, and 2% for *RH*, ranging from 0 to 99.9%). In particular, the MH-Z19 sensor has a response time in less than 60 seconds with an accuracy ± (50 ppm + 5% value) in a range from 0 to 5000 ppm. Figure 1 shows the schematics of the whole node where the reader can see the interconnection between the key components. Also Fig. 2 shows both layers of the designed PCB.

Such schematics has been layout in a PCB as part of the prototyping of the device. Figure 3 shows a photo of the node using the both mentioned MCUs: Amica with CP2102 chipset and Lolin with CH340 chipset. These nodes are connected via WiFi and send the information to the collection system via REST API.

#### 3.1.1 Calibration

NDIR sensors rely on an infrared light source and detector to measure the number of CO<sub>2</sub> molecules. But with aging, both the light source and the detector deteriorate, resulting in slightly lower CO<sub>2</sub> molecule counts, producing a drift in the readings. MH-Z19 sensor provides different options for calibration: a) auto-calibration according to the background, b) manual calibration referring to 400ppm, usually in a nitrogen environment, and c) digital zero-calibration (also referring to 400ppm), using fresh air. These calibration options have different pros and cons. In this case, the

**Table 1** Qualitative comparison of the proposed solution with other solutions

Work	Sensors	Technology	OTA update	Openness
[5]	Air pollution	WiFi	No	No
[9]	Particulate matter, CO <sub>2</sub> , TVOC, Air Temp and Rel.Hum	WiFi	No	No
[14]	PM2.5/PM10, VOCs, CO, CO <sub>2</sub>	LTE	No	No
[19]	Electrochemical (CO <sub>2</sub> , NO <sub>2</sub> , SO <sub>2</sub> , PM, NH <sub>3</sub> and toxic gases)	WiFi	No	No
[22]	Air pollution	Zigbee, WiFi, LTE and BLE	No	No
Our proposal	CO <sub>2</sub> , Temp, Rel. Hum	WiFi	Yes	Yes

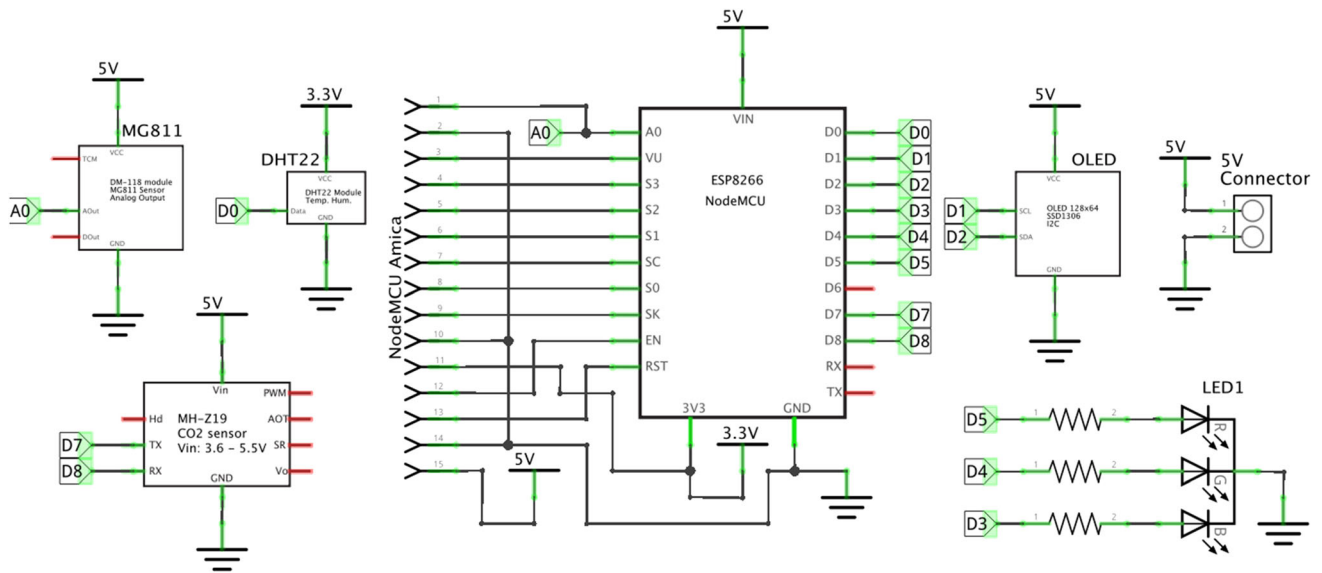


Fig. 1 Electronic schematic of the  $CO_2$ ,  $T$ ,  $RH$  node

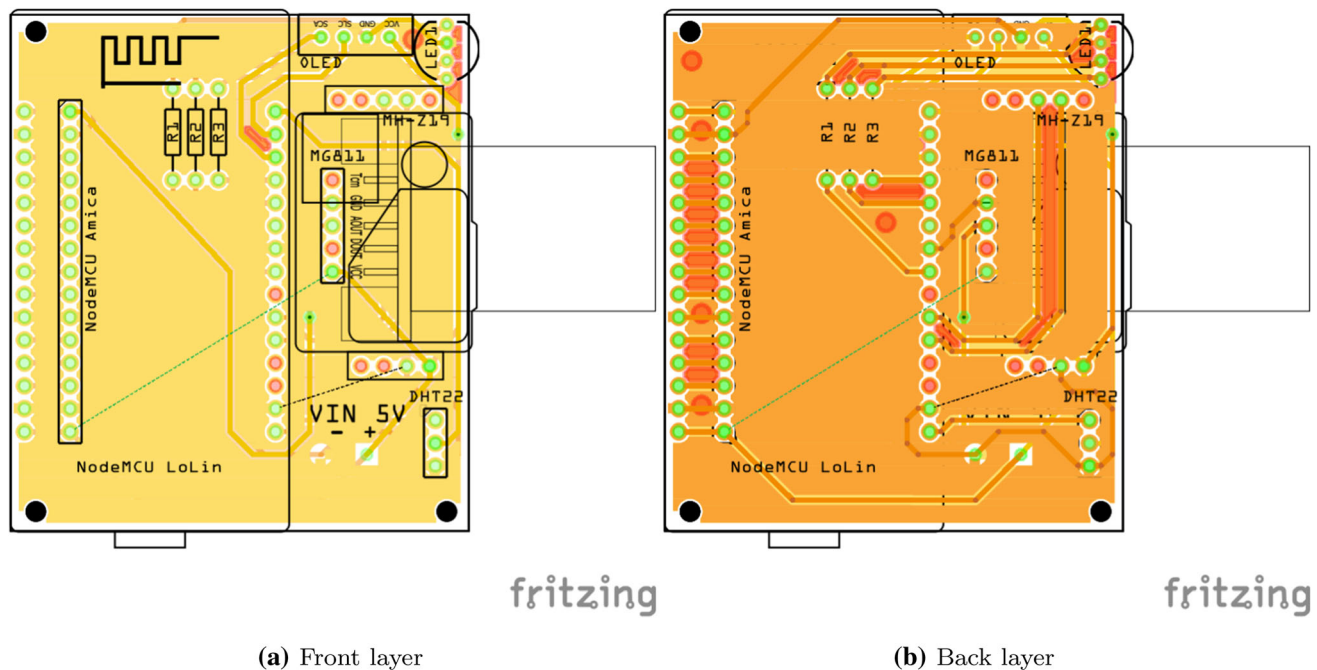


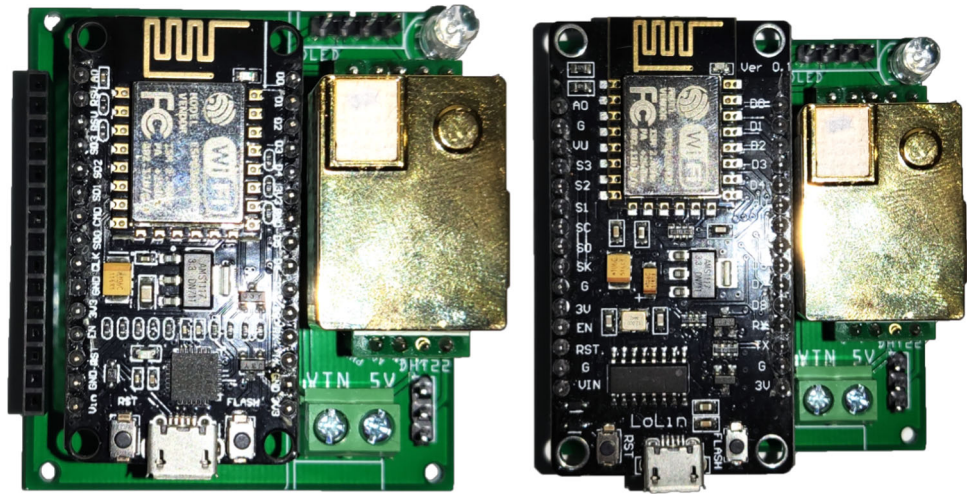
Fig. 2 Layers of the PCB

simplest one is the first one (a), based on the background, at the cost of a lower accuracy (around 50ppm plus 5% of the measurement value) that is a negligible amount in our case. This method is based on the fact that in a common environment,  $CO_2$  levels come back to 400ppm when there is no  $CO_2$  production for few hours, when the classroom is empty or during the night. That is because when there is nobody for a period of time of several hours,  $CO_2$  levels drop to a minimum. Also, we have considered option (c) or manual calibration, in which the node is located in an

environment with very low levels of  $CO_2$ , such as open spaces, far away from contamination, taking this reference as 400ppm. For this last option (c), optionally, the nodes have been designed to work with batteries, enabling the movement to suitable places to perform this calibration.

Finally it is worth mentioning that to combat the sensor drifts, during calibration of the sensor, multiple readings are taken. Then an average of these readings is calculated and the difference (or offset) between the new reading and the original reading when the sensor was originally

**Fig. 3** Photograph of the  $CO_2$ ,  $T$  and  $RH$  node with Amica and Lolin optional MCU



calibrated at the factory is stored in EPROM memory. Thus, this “offset” value is then automatically added or subtracted to later readings. This calibration is made via software.

In summary, our nodes combine a powering system, based on batteries (4xAA Energizer Max), and a software library to control the calibration options available for our NDIR  $CO_2$  sensor. Figure 4 shows a photograph with a mobile App deployed with the calibration functions programmed for this purpose. This photo was done while calibrating one node. For the calibration procedure, we need to connect the APP to the node and then set the low level (p.e. 400 ppm).

### 3.2 Architecture of the system

Figure 5 shows the overall system architecture proposed. The IoT Network is the segment where all the IoT nodes are deployed, in our case the classroom or place being monitored. Each IoT node is exposing an HTTP Server Rest API, used to perform the calibration of the sensors using our mobile application previously described. The IoT node has also a REST HTTP Client used to perform a periodic submission of the monitored information. The IoT nodes are connecting to a RPi via WiFi, sending information of  $CO_2$ ,  $T$  and  $RH$ . The RPi are deployed in the enterprise network segment acting as a gateway between the IoT network and the Internet. Notice that the RPi are considered optional devices in our infrastructure. They have been intentionally included to allow IoT devices to be deployed in the desired locations without the requirement to have direct Internet Wi-Fi coverage. However, if this limitation is acceptable for the concrete deployments (use case), the IoT devices are also capable to be directly connected to the Internet. The RPi are able to act as a gateway

for a significant number of IoT devices allowing a high-dense deployment. Our experiments have successfully achieved 40 IoT devices simultaneously connected to just one RPi.

In the Internet, we are making use of a mobile edge computing architecture. Such architecture is composed by at least two different network segments worth to be explained. The Edge and Core Network segment. The Edge segment, located close to the Enterprise network segment is where we have decided to perform the deployment of our Monitoring Server. The server is exposing a Server Rest API used by all the IoT devices to upload the sensed information. Such API is in charge of storing the monitored information into a MySQL Database. The same Server Rest API can be used to retrieve the information from a PC or smart phones application. In addition, this information can be used as an input to a control application towards the automation of the ventilation system via machine-to-machine communications. In the most simple scenario, this monitoring server can be located in a stand-alone server, however to deal with scalability we recommend to shift such monitoring server to the cloud and if after this we need to deal with even large scalability, when then shift to edge computing replicating the Server API and keeping load balancing and high performance optimizations for the database.

Once the information is collected from all the IoT devices, we have also developed an application that retrieved such information, allowing to show on real-time the monitored metrics. This application is currently developed by Android and has been installed in our classrooms to allow inhabitants to see the current status. The system is open-source and as such, further visualization tools can be developed to adapt to different execution environments (web, Windows, Linux, Apple Watch, iOS, etc).

As an added-value service, our architecture has another compute-intensive optional component, the Spatial

**Fig. 4** Photograph with the APP for calibration and led control node

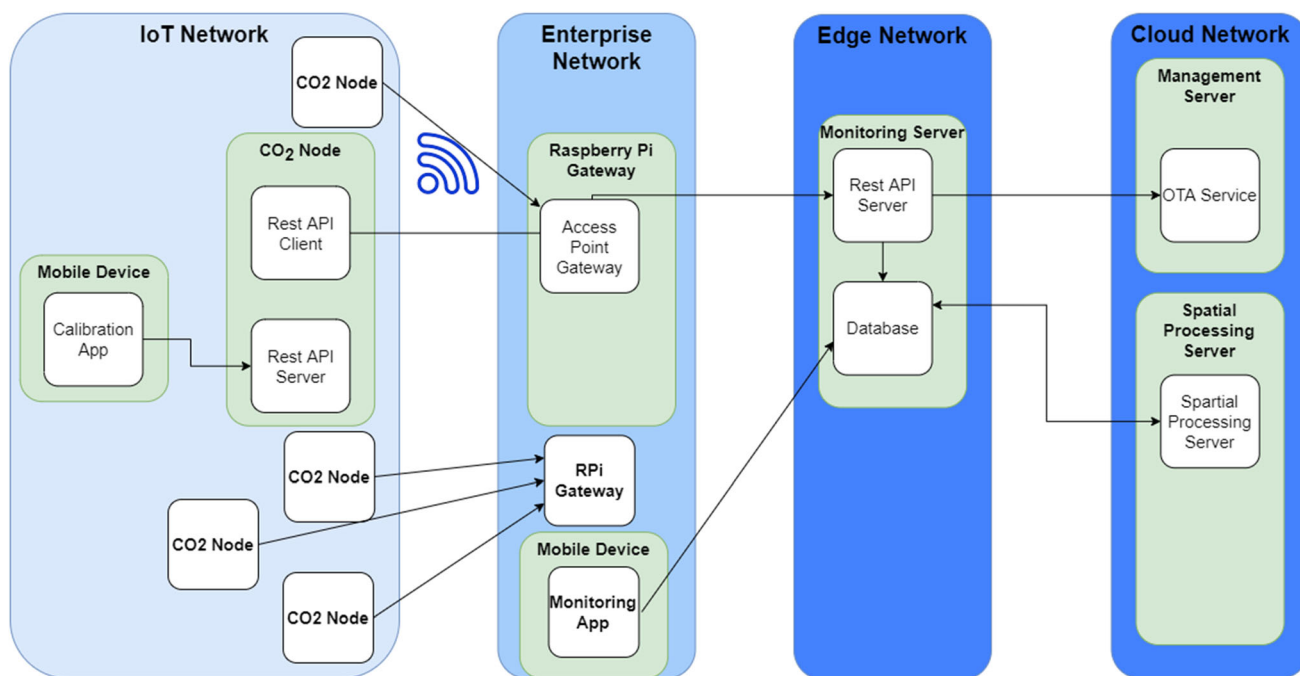
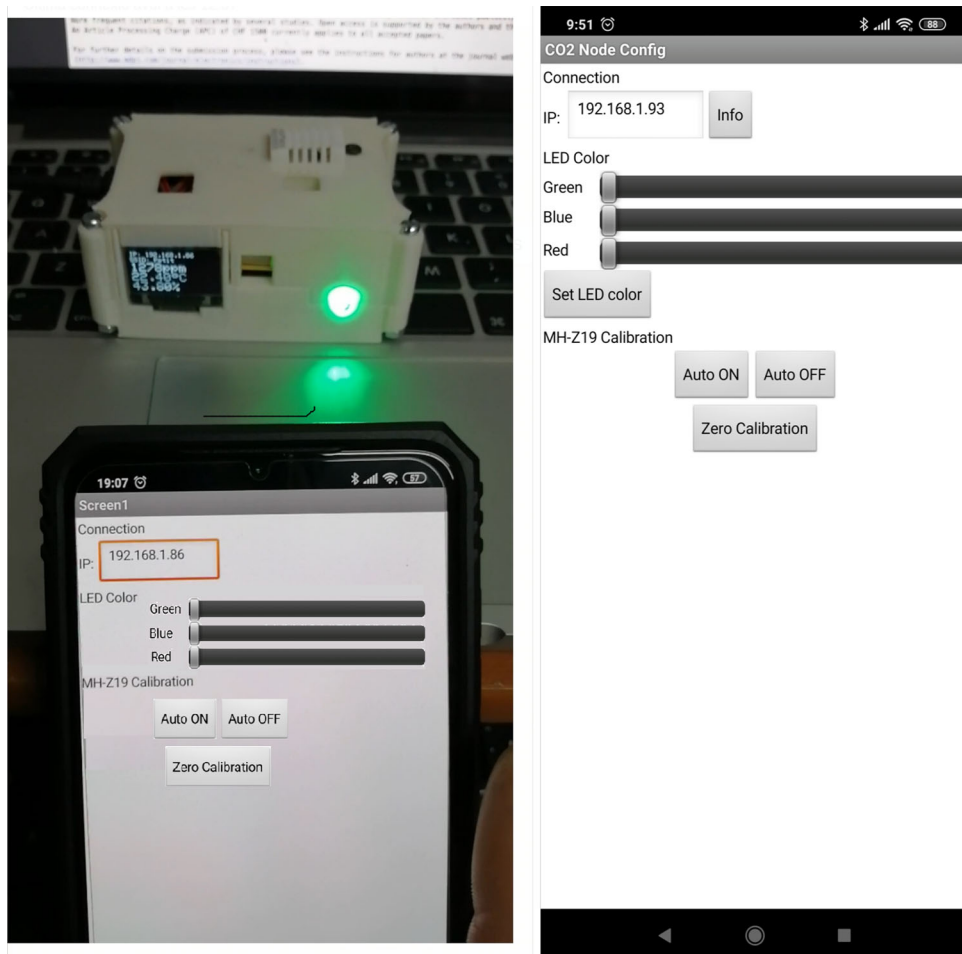


**Fig. 5** Schema of the system architecture

Processing Server. This server allow us to perform spatial interpolation to allow us to estimate the level of concentration of  $CO_2$  in every single point of the room by applying advance statistics, described in next subsection. This spatial processing server make use of the data gathered from all the IoT nodes and produces as an output the estimated interpolated value of the metrics for every of the positions of the room. Another optional added-value service compatible with our architecture is the usage of a Over-the-Air (OTA) firmware update server. This service allows us to perform the dynamic update of the firmware for all the IoT devices just in case more functionalities are pushed to the IoT devices without the need to re-deploy them. These additional compute-intensive added-value services are deployed in the Cloud to deal with scalability and compute-intensive requirements for large-scale deployments. It is worth to mention that the proposed architecture ranges from a very simple, client-server (2-layer) architecture until a 4-layer architecture able to deal with very large-scale deployments.

### 3.3 Spatial statistics

We have also studied the spatial statistical behavior of the information collected. To this end, we have chosen Kriging technique as a spatial interpolation method. The information from the  $CO_2$  concentration samples establish a data set based on measurement from different and specific locations. By denoting the determined value of the  $CO_2$  concentration measurements at a location  $x$  as  $C(x)$ , this data set is defined as  $\{C(x), x \in \mathcal{D}\}$ , where  $\mathcal{D}$  are all the locations of the modelling sets, following the Kriging technique [8].

The proposed model aims to forecast the value  $C(x_0)$  in any location  $x_0$ , specifically those in the validation set. The measurement reports contain information about the set of covariables included. Therefore in (1),  $C(x)$  is modeled as an average of each covariable involved in the process in the geographical area considered, plus some bounded spatial variability, which is explained by the short term process with spatial dependence.

$$C(x) = \mu(x) + \delta(x), \quad (1)$$

where  $\mu(x) = \mathbb{E}[C(x)]$  and  $\delta(x)$  is a stationary Gaussian process with zero mean, whose spatial dependence characterization is given by the variogram  $\gamma$  in (2). [10].

$$2\gamma(h) = \text{Var}[C(x+h) - C(x)] = \text{Var}[\delta(x+h) - \delta(x)], \quad (2)$$

where  $\text{Var}$  denotes the variance and  $h$  is an offset.

### 3.4 Public release

All the software and hardware presented in this paper has been released as open source available at <https://github.com/ETSE-UV/VentQ>. It includes, the hardware design and schematics together with the complete firmware of the IoT devices, the calibration application for the mobile application as well as the monitoring application to see the gathered metrics on real-time. The code of the monitoring server as well as the spatial processing server has been also released. For the OTA server, we are using an already existing ArduinoOTA open software<sup>1</sup>. The main intention is to make publicly accessible this low cost design to help controlling  $CO_2$  concentrations. This is a true open-software and open-hardware design.

## 4 Results and discussion

The evaluation of the performance of our system has been done by measuring in different scenarios, with a particular interest in classrooms during examination periods. Besides, we have evaluated the energy consumption of the nodes, in order to guarantee the life of the batteries, at least during 7 or 8 hours, approximately the duration of an exam including time intervals both at the beginning and at the end.

### 4.1 Measurements in daily situations

Prior to perform the real tests in classrooms during exam period and in order to check the proper operation of the nodes, we decided to perform different tests during daily activities, such as monitoring  $CO_2$  concentration in an office and in a bedroom. Notice that these two scenarios will remain with closed doors during the day.

Figure 6 a shows an office of approximately  $19.8 \text{ m}^3$ , used at least 10 hours a day by one person, turning on the heating system (by air conditioning) set to  $25^\circ\text{C}$  and turning it off at the end, keeping the room closed the whole time. The bedroom, shown in Fig. 6b, of  $26.25 \text{ m}^3$ , is only used for sleeping at night, by one person, turning on an electric radiator for a few minutes before going bed. Later, it remains closed the whole time, except early in the mornings when the window is opened 5 minutes for ventilation.

The results obtained in the office, as shown in Fig. 7, emphasize that the  $CO_2$  levels are reduced to low levels after during several hours while the office is empty, even with closed doors and windows. This confirms that the self-calibration of the nodes is possible, allowing us to calibrate

<sup>1</sup> <https://github.com/jandrassy/ArduinoOTA>

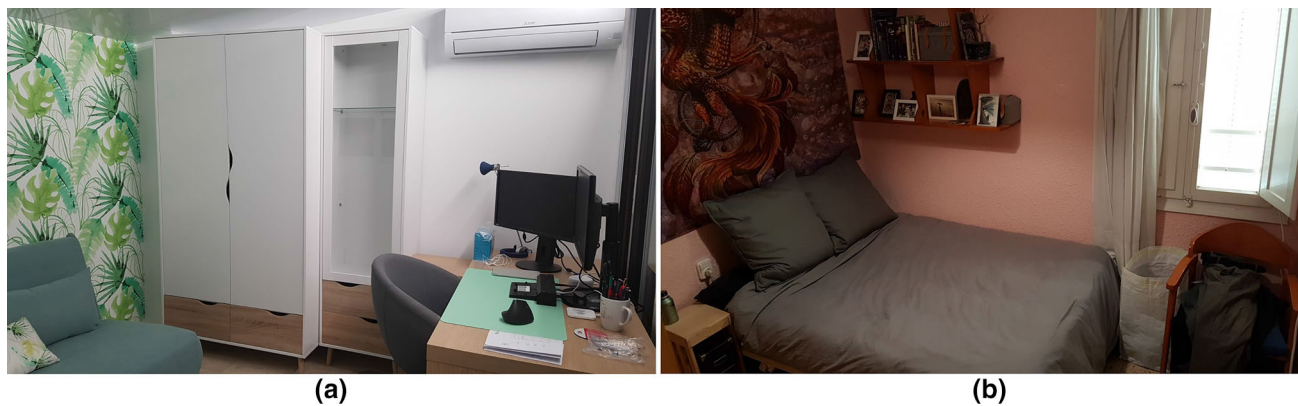


Fig. 6 Photograph of the daily scenarios analyzed

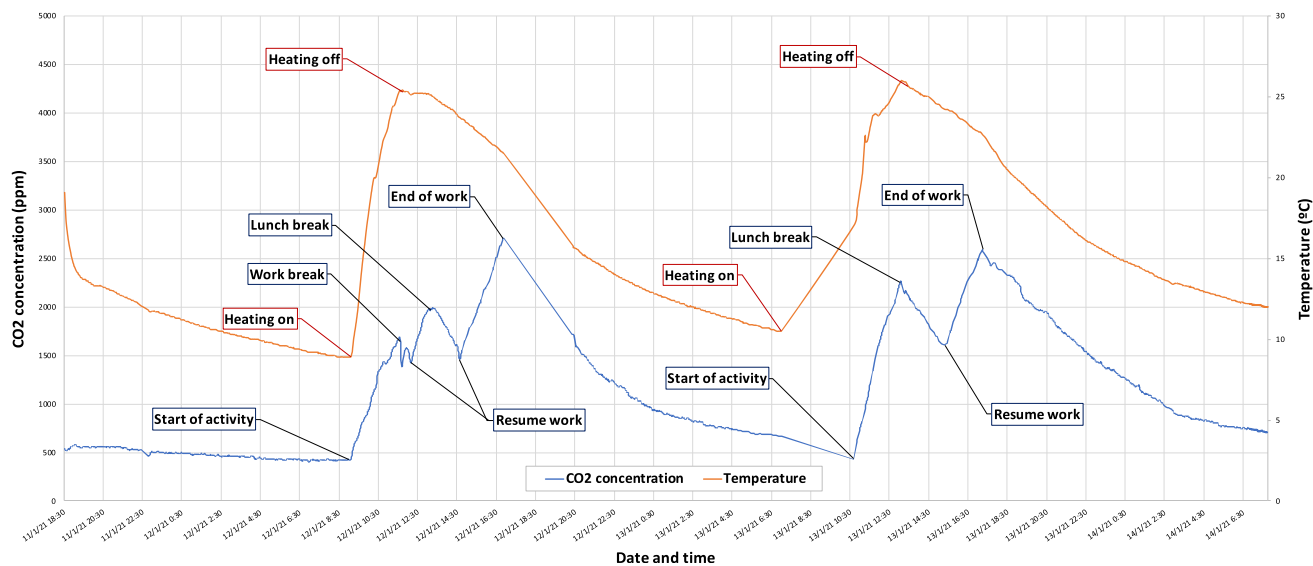


Fig. 7 CO<sub>2</sub> measurement in a office taken over several days

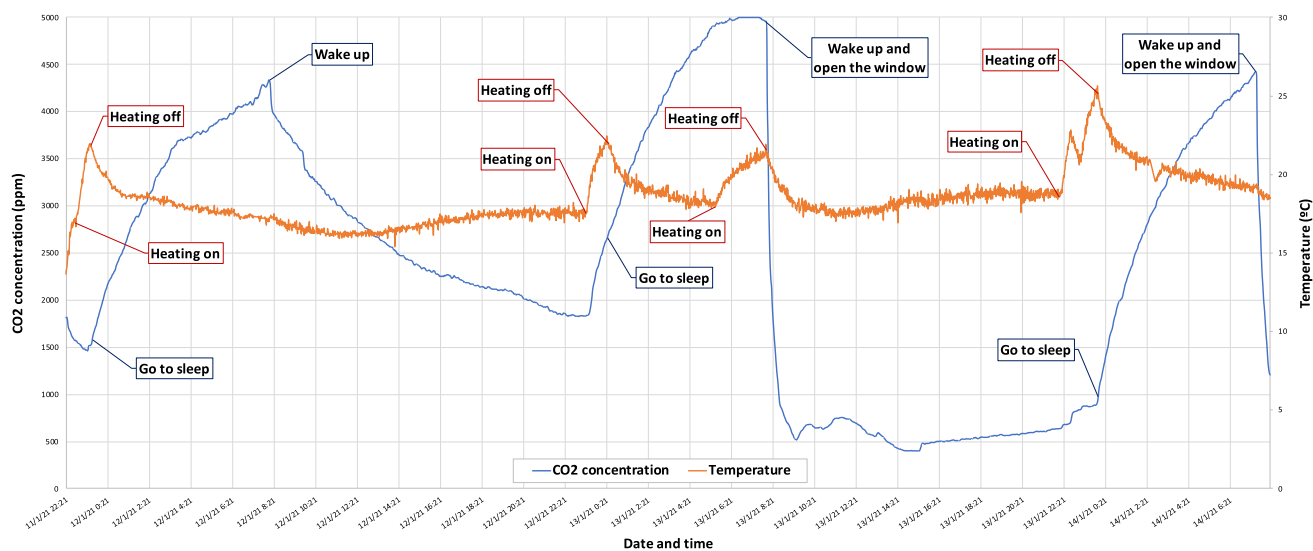


Fig. 8 CO<sub>2</sub> measurement in a bedroom taken over several days



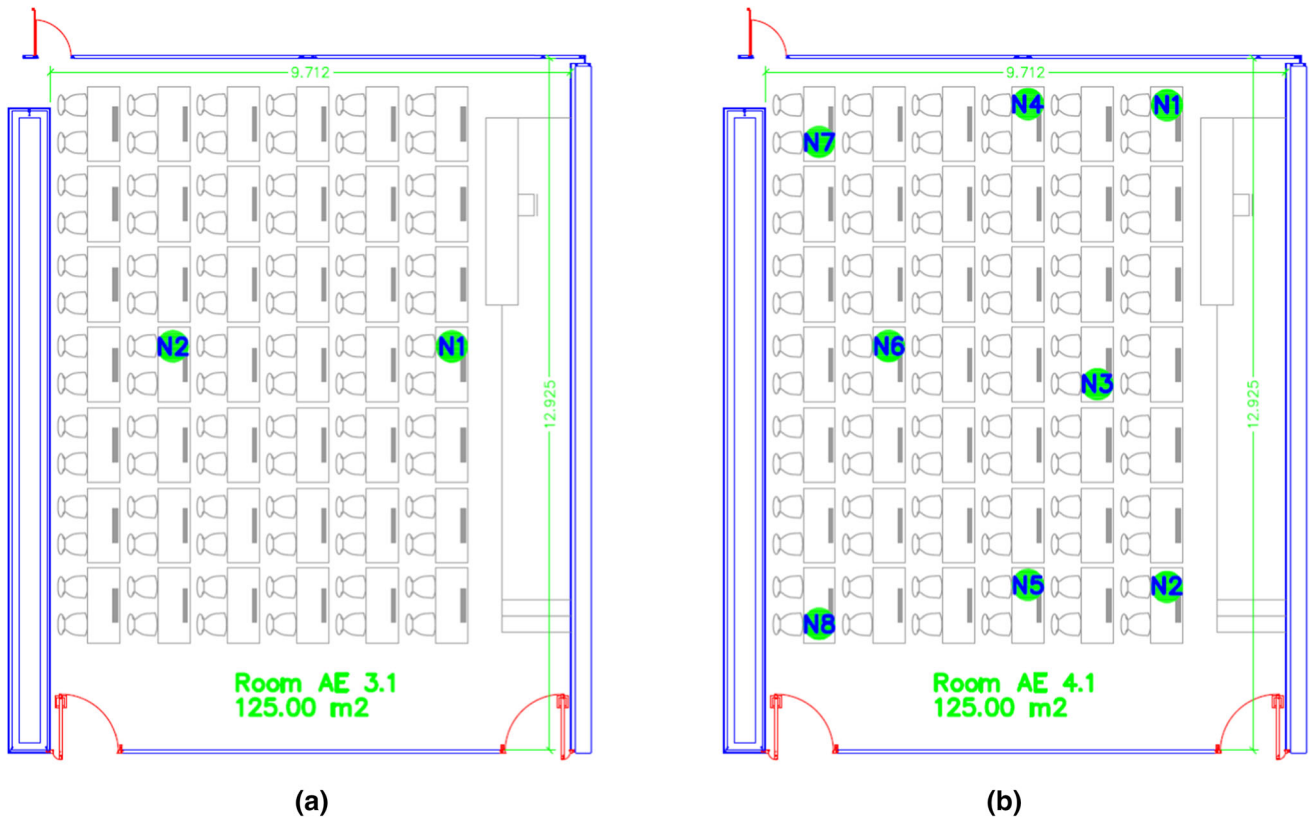
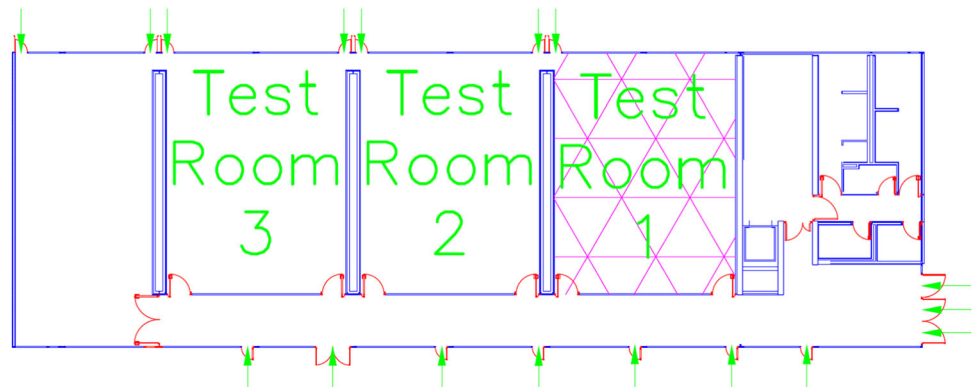


Fig. 9 Location of the nodes in classroom 3.1 (a) and classroom 4.1 (b) at the ETSE

Fig. 10 External air intakes in the building at the ETSE (green arrows show the external air input to the block 4 of the building)



in the same way classrooms when they are empty. During the breaks, when the office was empty but with the heating on,  $CO_2$  levels decreased and then increased again when the activity was resumed. This shows that this type of heating does not affect the measurements taken. Also notice that after lunch time, while being the heating system off, the increase in  $CO_2$  levels is similar to the ones when the heating system was on.

In the case of the bedroom, it can be seen in Fig. 8 that  $CO_2$  levels are much higher than those observed in the office. However these levels start to increase when the electric heating radiator is switched on, despite the fact that

anybody remains in the room, which means that this type of heating system affects the concentration of  $CO_2$  in the environment. After the first night, the window was not opened for ventilation, so it can be seen how  $CO_2$  levels slowly dropped to their initial levels. However, after the second and third night, when the window was opened for ventilation, the levels dropped to a minimum in a very short time (in the order of minutes), which demonstrates how easy and quick a closed space can be adequately ventilated.

**Fig. 11** Photograph of the classroom 4.1 during the test

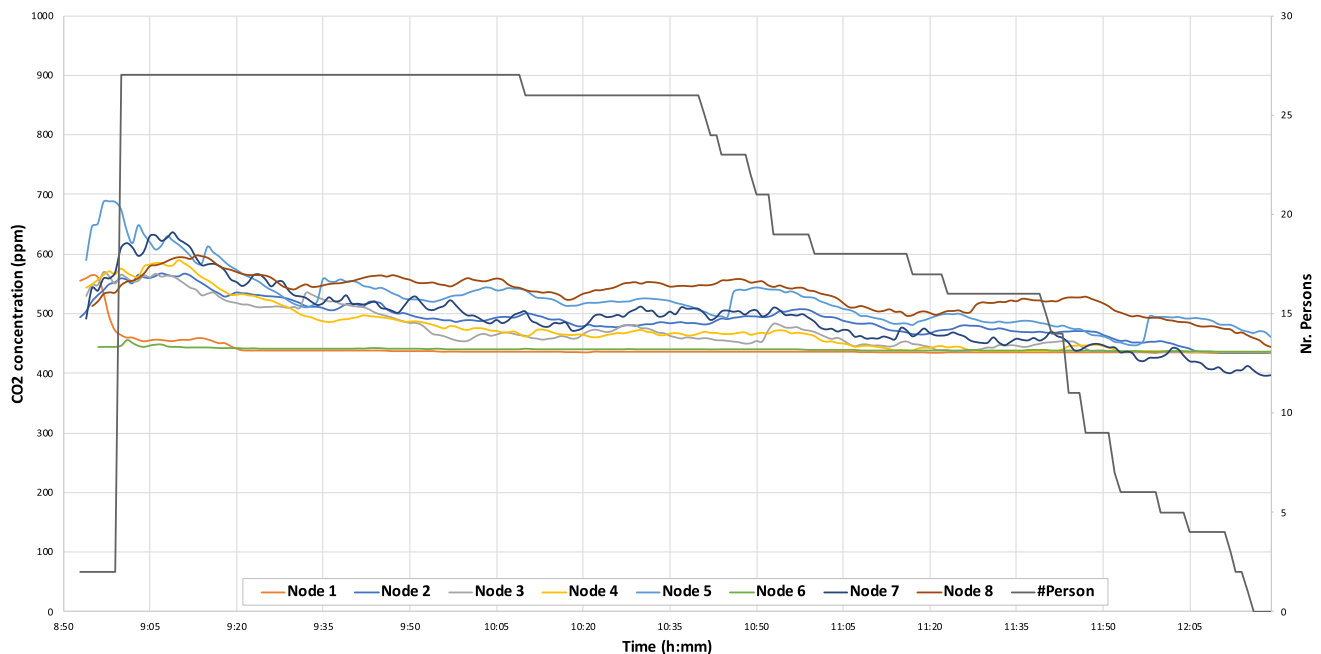


**Fig. 12**  $CO_2$  measurement in room 4.1 at ETSE during an exam in January with 8 nodes vs. number of persons in the room (doors and windows were open)

## 4.2 Measurements in the examination period

In order to test our system in a field evaluation, we have made some measurements during different exams in the examination period in December 2020 at room number 3.1 and January 2021 at room number 4.1 in the ETSE of the University of Valencia. Figure 9 shows the location of the nodes in the classroom 3.1 (Fig. 9a) and 4.1 (Fig. 9b).

A photograph can be seen during the measurements in Fig. 11. As these nodes are equipped with batteries, they can be located anywhere. Also, as shown in this figure,

doors and windows are opened, ensuring a good ventilation, following the COVID-19 instructions.

Both classrooms are located in different buildings with identical distribution. Also, they have multitude of air inlets from the outside, as we can see in Fig. 10, marked with green arrows. These inlets promote a good ventilation inside the classroom, ensuring low levels of  $CO_2$ . The location of the classrooms inside the building is marked as Test Room 1.

In Fig. 11, we can see a photograph during an exam in January 2021. Figure 12 shows the time evolution of  $CO_2$  concentration measured using eight different nodes. In both

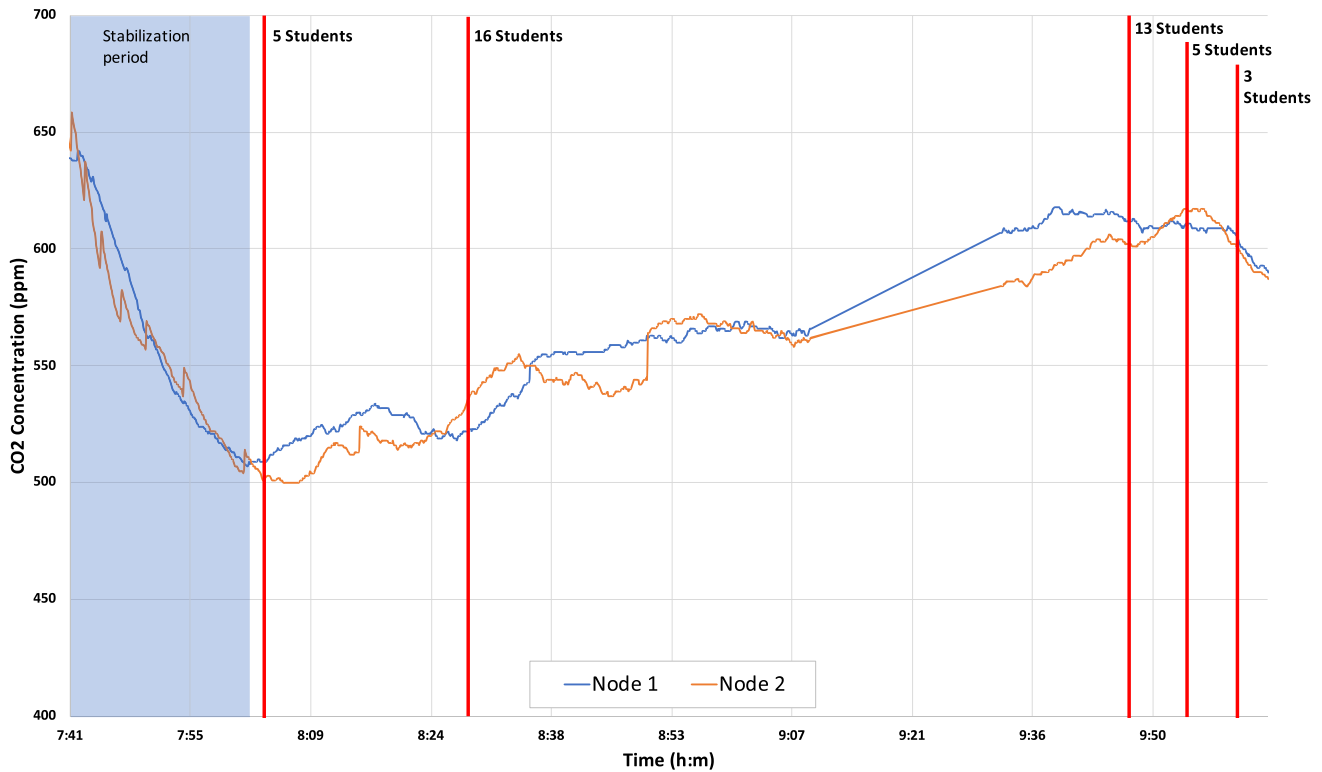


Fig. 13 CO<sub>2</sub> measurement in a classroom during an exam in December with 2 nodes

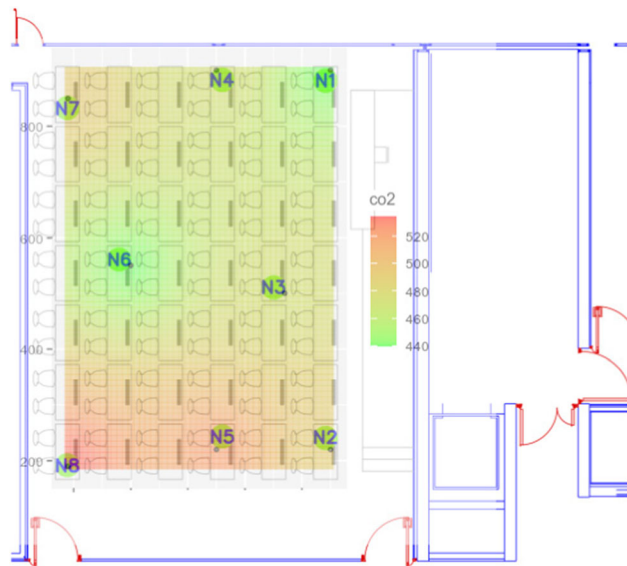


Fig. 14 Spatial statistic representation of mean values of CO<sub>2</sub> concentration in room 4.1 at ETSE during an exam in January with 8 nodes

cases, the natural ventilation (due to open doors and windows) allows to keep the CO<sub>2</sub> concentration controlled, reducing the risks of COVID-19 contagions. These results show the correct behavior of the proposed system. In addition, Fig. 13 shows a line of the evolution of CO<sub>2</sub>

concentration from two nodes during an exam in December 2020. In this figure, we can see a slight rise of the concentration, while the number of students increases. As the room is well ventilated, the CO<sub>2</sub> levels are not too high and under control.

### 4.3 Spatial statistics

Figure 14 shows the spatial statistic study of the average of CO<sub>2</sub> concentration, using Kriging technique [8, 10, 21, 26] during the exam in January 2021. This method allows to predict (by means of statistical interpolation) the values inside the defined grid. In this case, we have used Ordinary Kriging [29] to compute the evolution of the spatial distribution of CO<sub>2</sub> concentration in the classroom. The video provided as supplementary material shows the time evolution per minute of the CO<sub>2</sub> concentration during the exam. It shows how well the class is ventilated during the exam

### 4.4 Energy consumption performance evaluation

Now, we evaluate the energy consumption of the proposed nodes with two different configurations: (a) by using the MCU with the MH-Z19 and DHT22 sensors, together with a RGB led and an OLED screen and (b) by using both

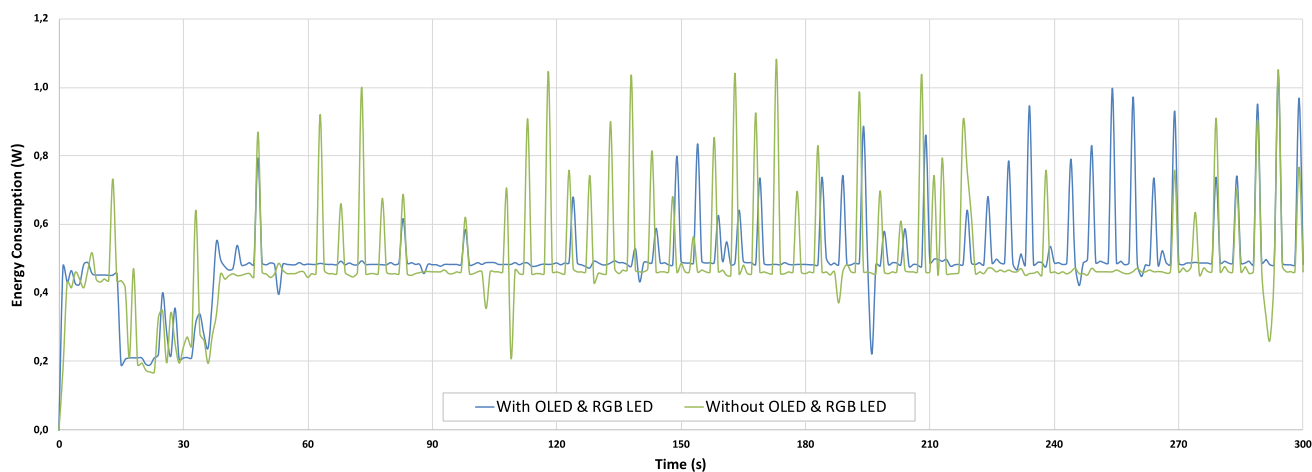


**Fig. 15** Energy consumption of the measurement and communication process in the node

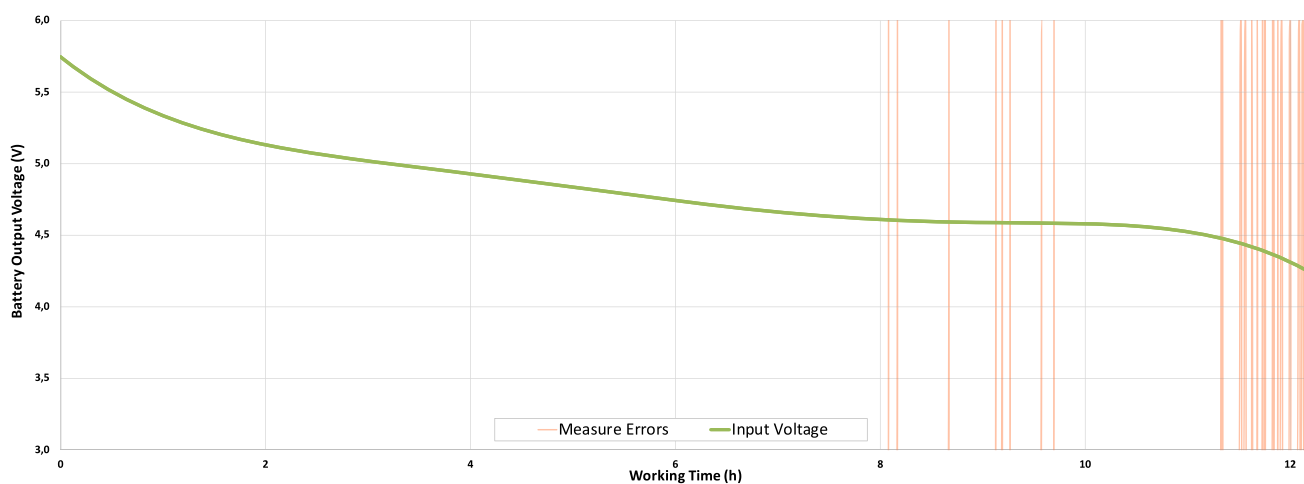


**Fig. 16** Operation and duration of the node with batteries

sensors without the RGB led and the OLED screen. To this end, we use a USB power-meter UM34C [25].

Figure 15 shows the initialization of the node, with a starting sleep mode, and a measurement period in one node, with both configurations (a) in green color and (b) in blue color. We can observe from this figure that the consumption of the OLED screen and RGB led is very low, around 0.03W in average.

Also from Fig. 15, we can see different peaks corresponding to the measurement period of the MH-Z19 sensor, since the Infrared (IR) source of the NDIR switches on every 5 s during 400 ms. Therefore, we can conclude that these peaks correspond to the energy used to switch this IR lamp on. It must be noticed that these nodes have been designed to operate with 4 AA batteries for short-term measurement campaigns, in places where direct power supply is not possible. Therefore, these tests have been carried out to verify the duration of the nodes when measuring.

Energizer Max E91 type AA batteries [6] have been used and the node has been configured to take and send samples every 5 seconds with the display and RGB led on. Both the samples sent and the voltage supplied by the batteries have been monitored. Figure 16 shows the output voltage of the batteries and the errors in data readings. As it can be observed, errors start appearing sporadically after 8 hours of uninterrupted operation when the voltage drops to 4.6V and they continue working during 11 hours more, when the voltage drops to 4.5V. Finally the node stops working after more than 12 hours when the voltage drops below 4.2V.

## 5 Conclusions

In this work we have developed a fully operative open-hardware and open-software fully operational IoT system and architecture to measure  $CO_2$  concentration,

temperature and relative humidity. This system is fully scalable and automatically upgradeable, thanks to the OTA updating function. The building cost of this system is low-cost, less than 100\$.

This system has been tested in different environments: at work, at home and in class during different exams. The measurements taken shows full range operation (limited only by the sensor performance), allowing us to show perfectly the temporal evolution of the  $CO_2$  concentration.

In order to study the spatio-temporal evolution of the  $CO_2$  concentration measured in different situations, the architecture has been empowered with cloud-based processing capabilities to achieve Kriging technique to perform spatial interpolation of the metrics.

Finally, the energy consumption of the developed nodes has been also evaluated in each part of the circuit, lasting till 12 hours of continuous monitoring. As a future work, we are going to develop the node using a Fipy MCU which will allow 5G communication with these nodes. As this is a modular system that can be improved and upgraded (due to its openness). The use of other sensors such as PM3005 (for monitoring PM2.5 or PM10), TVOC and other gasses can be a matter of improvement by adding I2C, SPI or other interfaces to the sensing module. We also would like to explore ultra low power consumption real-time processors to extend the duration of the system with the same number of batteries.

**Supplementary Information** The online version contains supplementary material available at <https://doi.org/10.1007/s11276-021-02799-5>.

**Acknowledgements** This work was partially funded by the European Commission Horizon 2020 5G-PPP Program under project H2020-ICT-2020-2/101016941: “5G INDUCE: OpenCooperative 5G Experimentation Platforms for The Industrial Sector NetApps” and by the Generalitat Valenciana under the grant number AEST/117/2020 and the Universitat de Valencia for the grant number UV-INV-AE-1544281.

**Funding** Open Access funding provided thanks to the CRUE-CSIC agreement with Springer Nature.

## Declarations

**Conflict of interest** The authors declare that they have no conflict of interest.

**Open Access** This article is licensed under a Creative Commons Attribution 4.0 International License, which permits use, sharing, adaptation, distribution and reproduction in any medium or format, as long as you give appropriate credit to the original author(s) and the source, provide a link to the Creative Commons licence, and indicate if changes were made. The images or other third party material in this article are included in the article’s Creative Commons licence, unless indicated otherwise in a credit line to the material. If material is not included in the article’s Creative Commons licence and your intended use is not permitted by statutory regulation or exceeds the permitted

use, you will need to obtain permission directly from the copyright holder. To view a copy of this licence, visit <http://creativecommons.org/licenses/by/4.0/>.

## References

1. Adafruit Industries: DHT22 temperature & humidity sensor (2016). URL: <http://www.adafruit.com/datasheets/DHT22.pdf>. (Accessed: 10/01/2021).
2. Arroyo, P., Herrero, J. L., Suárez, J. I., & Lozano, J. (2019). Wireless sensor network combined with cloud computing for air quality monitoring. *Sensors (Switzerland)*. <https://doi.org/10.3390/s19030691>.
3. Azuma, K., Yanagi, U., Kagi, N., Kim, H., Ogata, M., & Hayashi, M. (2020). Environmental factors involved in SARS-CoV-2 transmission: Effect and role of indoor environmental quality in the strategy for COVID-19 infection control. *Environmental Health and Preventive Medicine*. <https://doi.org/10.1186/s12199-020-00904-2>.
4. Bhagat, R. K., Wykes, M. S. D., Dalziel, S. B., & Linden, P. F. (2020). Effects of ventilation on the indoor spread of COVID-19. *Journal of Fluid Mechanics*. <https://doi.org/10.1017/jfm.2020.720>.
5. Boubrima, A., Bechkit, W., & Rivano, H. (2017). Optimal WSN deployment models for air pollution monitoring. *IEEE Transactions on Wireless Communications*. <https://doi.org/10.1109/TWC.2017.2658601>.
6. Brands, E. Energizer e91 datasheet (2020). <http://data.energizer.com/pdfs/e91.pdf> (Accessed: 17/01/2021).
7. Chaabouni, S., & Saidi, K. (2017). The dynamic links between carbon dioxide (CO<sub>2</sub>) emissions, health spending and GDP growth: A case study for 51 countries. *Environmental Research*. <https://doi.org/10.1016/j.envres.2017.05.041>.
8. Cressie, N. (1993). *Statistics for spatial data*. New York: John Wiley.
9. Demanega, I., Mujan, I., Singer, B. C., Anelkovic, A. S., Babich, F., & Licina, D. (2021). Performance assessment of low-cost environmental monitors and single sensors under variable indoor air quality and thermal conditions. *Building and Environment*. <https://doi.org/10.1016/j.buildenv.2020.107415>.
10. Diblasi, A., & Bowman, A. (2001). On the use of the variogram in checking for independence in spatial data. *Biometrics*, 57, 211–218.
11. Duan, R. R., Hao, K., & Yang, T. (2020). Air pollution and chronic obstructive pulmonary disease. *Chronic Diseases and Translational Medicine*. <https://doi.org/10.1016/j.cdtm.2020.05.004>.
12. Espressif Systems: Nodemcu datasheet (2013). URL: [https://www.elecrow.com/download/ESP8266\\_Specifications\\_English.pdf](https://www.elecrow.com/download/ESP8266_Specifications_English.pdf). (Accessed: 01/02/2021).
13. European Centre for Disease Prevention and Control: Heating, ventilation and air-conditioning systems in the context of COVID-19. Tech. rep., European Union, Stockholm (2020). <https://www.ecdc.europa.eu/en/publications-data/heating-ventilation-air-conditioning-systems-covid-19>.
14. Jo, J., Jo, B., Kim, J., Kim, S., & Han, W. (2020). Development of an IoT-based indoor air quality monitoring platform. *Journal of Sensors*, 2020, 8749764. <https://doi.org/10.1155/2020/8749764>.
15. Liu, Z., Ciais, P., Deng, Z., et al. (2020). Near-real-time monitoring of global CO<sub>2</sub> emissions reveals the effects of the COVID-19 pandemic. *Nature Communications*. <https://doi.org/10.1038/s41467-020-18922-7>.

16. McKinney, K. R., Gong, Y. Y., & Lewis, T. G. (2006). Environmental transmission of SARS at amoy gardens. *Journal of Environmental Health*, 68, 26–52.
17. Mialdea-Flor, I., Segura-Garcia, J., Felici-Castell, S., Garcia-Pineda, M., Alcaraz-Calero, J. M., & Navarro-Camba, E. (2019). Development of a low-cost IoT system for lightning strike detection and location. *Electronics (Switzerland)*. <https://doi.org/10.3390/electronics8121512>.
18. Minguillón, M.C., Querol, X., Felisi, J.M., & Garrido, T. Guía para ventilación de las aulas CSIC (2020). 10.20350/DIGITALCSIC/12677. <https://digital.csic.es/handle/10261/221538>.
19. Nagaraj, S., & Biradar, R.V. Applications of wireless sensor networks in the real-Time ambient air pollution monitoring and air quality in metropolitan cities-A survey. In: Proceedings of the 2017 international conference on smart technology for smart nation, SmartTechCon 2017 (2018). 10.1109/SmartTechCon.2017.8358594.
20. NodeMCU documentation: Over-the-air updating (2018). URL: <https://nodemcu.readthedocs.io/en/release/build/>. (Accessed: 10/01/2021).
21. Pastor-Aparicio, A., Segura-Garcia, J., Lopez-Ballester, J., Felici-Castell, S., Garcia-Pineda, M., & Perez-Solano, J. J. (2020). Psychoacoustic annoyance implementation with wireless acoustic sensor networks for monitoring in smart cities. *IEEE Internet of Things Journal*. <https://doi.org/10.1109/JIOT.2019.2946971>.
22. Patil, D., Thanuja, T. C., & Melinamath, B. C. (2018). Air pollution monitoring system using wireless sensor network (WSN). In V. Balas, N. Sharma, & A. Chakrabarti (Eds.), *Data management, analytics and innovation* (pp. 391–400). Singapore: Springer.
23. Perez, A. O., Bierer, B., Scholz, L., Wöllenstein, J., & Palzer, S. (2018). A wireless gas sensor network to monitor indoor environmental quality in schools. *Sensors (Switzerland)*. <https://doi.org/10.3390/s18124345>.
24. Petersen, S., Jensen, K. L., Pedersen, A. L., & Rasmussen, H. S. (2016). The effect of increased classroom ventilation rate indicated by reduced CO2 concentration on the performance of schoolwork by children. *Indoor Air*. <https://doi.org/10.1111/ina.12210>.
25. Ruideng. UM34C User Manual (2020). <http://ruidengeji.com/inst/UM34C.pdf> (Accessed: 10/01/2021).
26. Segura-Garcia, J., Navarro-Ruiz, J., Perez-Solano, J., Montoya-Belmonte, J., Felici-Castell, S., Cobos, M., & Torres-Aranda, A. (2018). Spatio-temporal analysis of urban acoustic environments with binaural psycho-acoustical considerations for IoT-based applications. *Sensors*, 18, 690.
27. Seppänen, O. A., Fisk, W. J., & Mendell, M. J. (1999). Association of ventilation rates and CO2 concentrations with health and other responses in commercial and institutional buildings. *Indoor Air*, 9(4), 226–252. <https://doi.org/10.1111/j.1600-0668.1999.00003.x>.
28. Turanjanin, V., Vučec, B., Jovanović, M., Mirkov, N., & Lazović, I. (2014). Indoor CO2 measurements in Serbian schools and ventilation rate calculation. *Energy*, 77, 290–296. <https://doi.org/10.1016/j.energy.2014.10.028>.
29. Wackernagel, H. (2003). *Ordinary kriging* (pp. 79–88). Berlin: Springer.
30. Zhang, J. (2020). Integrating IAQ control strategies to reduce the risk of asymptomatic SARS CoV-2 infections in classrooms and open plan offices. *Science and Technology for the Built Environment*, 26(8), 1013–1018. <https://doi.org/10.1080/23744731.2020.1794499>.
31. Zhengzhou Winsen Electronics Technology Co. Ltd. MH-Z19B NDIR CO2 sensor for indoor air quality monitoring–Winsen (2018). <https://go.uv.es/dulGL49>, (Accessed: 20/01/2021).

**Publisher's Note** Springer Nature remains neutral with regard to jurisdictional claims in published maps and institutional affiliations.



**Rafael Fayos-Jordan** received the B.S. Degree in Telematics Engineering from the University of Valencia in 2018. He is currently in the last year of master degree in Web Technology, Cloud Computing and Mobile Applications and working as researcher in Department of Computer Science, University of Valencia. His interest is in the IoT platforms and node management, cloud computing and network management.



**Jaume Segura-Garcia** received the M.Sc. and Ph.D. degrees in physics from the University of Valencia, Valencia, Spain, in 1998 and 2003, respectively. After completing his Ph.D. study, he was with the Robotics Institute, University of Valencia, where he was involved in several projects related to intelligent transportation systems. Since 2008, he has been with the Department of Computer Science, University of Valencia, where he is currently an Associate Professor. He has been a Visiting Researcher with multiple European research centres. He has co-authored over 90 publications at national and international journals, book chapters, and conferences. He was on the Organizing Committee of several national and international conferences, including the International Workshop on Virtual Acoustics (2011). He is a member of the Spanish Acoustics Society and the European Acoustics Association.



**Antonio Soriano-Asensi** was born in Benaguasil, Valencia, Spain, in 1978. He received the Licenciado degree in physics and the Ph.D. degree from the University of Valencia, Valencia, in 2001 and 2007, respectively. He has worked as a Postdoctoral Research at the Spanish National Research Council (CSIC), the Universitat Politècnica de Valencia, and the Universitat Jaume I. Since 2017, he has been an Associate Professor with the Department of Informatics, University of Valencia. His research interests include computer networks and robotics.



**Santiago Felici-Castell** received the M.Sc. and Ph.D. degrees in telecommunication engineering from the Polytechnical University of Valencia, Valencia, Spain, in 1993 and 1998, respectively. He is currently an Associate Professor with the University of Valencia, Valencia. His research has focused on networking, communication systems, and multiresolution techniques for data transmission with quality of service. He is also a Cisco Systems Certified

Instructor, and has authored over 25 technical papers in international journals and conferences.



**Jose M. Felisi** was born in Villar, Valencia, in 1976. He received his Bachelor degree in Chemistry Engineering in 2002. He is manager of the company G-Agua since its foundation in 2006. He is also leading the Mesura association, devoted to obtaining and processing data from many sources in different parts of the Valencia Community and applying open-science principles. His main interests are oriented to chemical processes, environmental monitor-

ing, sensing and IoT.



**Jose M. Alcaraz-Calero** (Senior Member, IEEE) received the Ph.D. degree in computer Science from the University of Murcia. He is currently a Full Professor in next-generation networks and security with the University of the West of Scotland. He is the Technical Co-Coordinator of the EU H2020 5G-PPP SELFNET and SliceNet projects and a Co-Principal Investigator of the EU H2020 5G INDUCE and 6G BRAINS projects. His professional inter-

ests include network cognition, management, security and control, service deployment, automation and orchestration, and 5G mobile networks.